Evaporation Pressure Drop Characteristics with R-22 in the Plate and Shell Heat Exchangers

Jae-Hong Park*, Moo-Gyo Seo**, Ki-Baik Lee*** and Young-Soo Kim*

Key words: Plate and shell heat exchanger, Pressure drop, Refrigerant, Vapor quality

Abstract

In this study, evaporation pressure drop experiments were conducted with two types of plate and shell heat exchangers (P&SHE) using R-22. An experimental refrigerant loop has been established to measure the evaporation pressure drop of R-22 in a vertical P&SHE. The flow channels were formed by stacking three plates having a corrugated channel of a chevron angle of 45 deg. The R-22 flows down in one channel exchanging heat with the hot water flowing up in the other channel. The effect of the refrigerant mass flux, average heat flux, system pressure and vapor quality were explored in detail. During the experiment, the quality change between the inlet and outlet of the refrigerant channel ranges from 0.03 to 0.15. The present data showed that two types of P&SHE have similar trends. The pressure drop increases with the vapor quality for both types of P&SHE. At a higher mass flux, the pressure drop is higher for the entire range of the vapor quality. Also, the increase in the average heat flux increases the pressure drop. Finally, at a higher system pressure, the pressure drop is found to be slightly lower compared to the lower system pressure.

Nomenclature

D_h : hydraulic diameter [m]

f : friction factor

g : acceleration due to gravity [m/s^2]

G : mass flux [kg/m^{2}s]

L : length from center of inlet port to center of exit port [m]

u : velocity [m/s]

w : width of the plate, $2/3D$ [m]

x : vapor quality

Greek symbols

ΔP : pressure drop

Δx : vapor quality change in the exchanger

ρ : density [kg/m^3]

υ : specific volume [m^3/kg]

* Department of Refrigeration Engineering, Graduate School of Pukyong National University, Pusan 608-737, Korea

** Samsung Electronics Co., LTD, Airconditioner R&D, Suwon 442-742, Korea

*** Department of Automative Fabrication, Changwon Polytechnic College, Changwon 641-772, Korea

μ : viscosity [$N \cdot s/m^2$]

Subscripts

g : vapor phase
h : hot side
l : liquid phase
m : average value
p : pre-heater
r : refrigerant
TP : two phase
w : water

1. Introduction

In view of space saving, the design of more compact heat exchangers is relatively important. Also, to meet the demand for saving energy and resources today, manufacturers are trying to enhance efficiency and reduce the size and weight of heat exchangers. Over the past decade, there has been tremendous advancement in the manufacturing technology of high efficient heat exchangers. This has allowed the use of compact and high performance heat exchangers. Consequently, the use of compact and high performance heat exchanger will become popular in the design of HVAC heat exchangers. Normally, these heat exchangers are used in the two phase system for evaporation and condensation. In the design and analysis of the two phase system within this heat exchanger, it is necessary to understand the flow field and frictional characteristic of the two phase system.

When compared with the well established shell and tube heat exchangers, the plate heat exchangers (PHE) show a lot of advantages like high NTU values, compactness, low cost, multi duties and reduced fouling etc. PHEs have been widely used in food processing, chemical reaction processes, and other industrial applications for many decades. The advantage of using PHE was clearly indicated in the studies from Williams[1] and Kerner.[2] Particularly, in the last 20 years PHEs have been introduced to the refrigeration and air conditioning systems as evaporators or condensers for their high efficiency and compactness.

The plate and shell heat exchanger (P&SHE) is different from the conventional PHE. The plates that have oblique line grooves are circular, and stacked together in contrary arrangements, which are enclosed a cylindrical shell. Operating temperature rises up to 350℃, and pressure can be achieved to 10 MPa. Although P&SHE is apparently different from the conventional rectangular plate exchanger, the underlying flow channels through the exchanger are the same as the conventional PHE. The P&SHE is being introduced to the refrigeration and air conditioning systems as evaporators or condensers for their high efficiency and compactness.

Unfortunately, some studies about P&SHE and PHE have been reported in the open literature focusing on the single phase liquid heat transfer.[3-9] There is also little data available for the design of P&SHE used as evaporators and condensers.

In the present study, the characteristics of evaporation pressure drop for R-22 flowing in the P&SHE were explored experimentally to set up data base for the design of the P&SHE.

2. Experimental apparatus & procedures

2.1 Experimental apparatus

The heat transfer plates and experimental system established to investigate the evaporation pressure drop characteristics of R-22 are shown in Fig. 1 and 2. The experimental system was constituted with test section, refrigerant loop, water loop and a data acquisition unit.

Refrigerant R-22 is circulated in the refri-

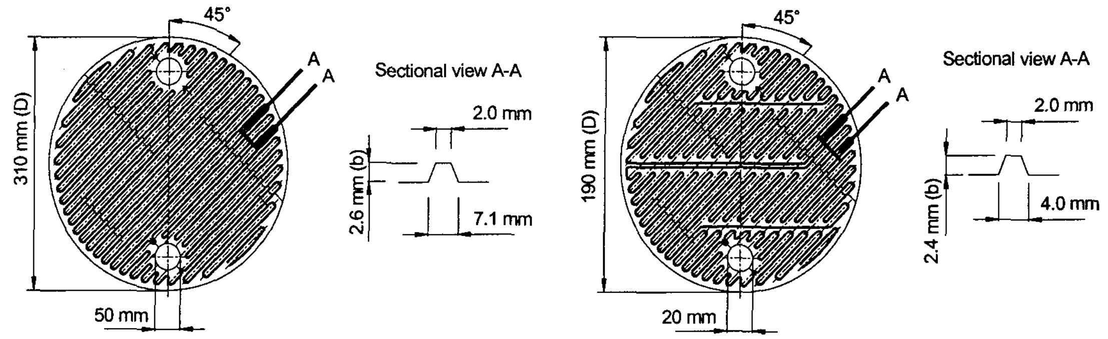

(a) Type A (b) Type B

Fig. 1 Schematic diagram of plate and shell heat exchangers.

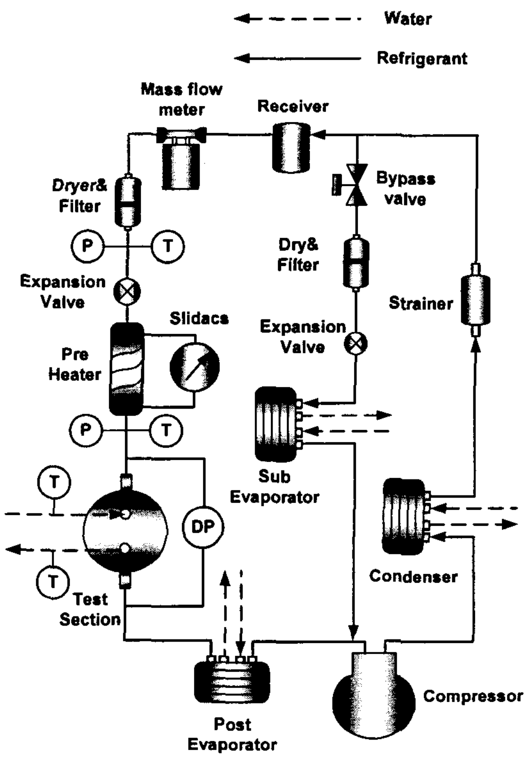

Fig. 2 Schematic diagram of the experimental system.

gerant loop. In order to obtain different test conditions of R-22 including vapor quality, system pressure and imposed heat flux in the test, we need to control the temperatures and flow rates of the working fluids in the water loop.

Table 1 Configurations of the *P&SHE*

Plate material	SUS 304
Shell material	Steel
Plate thickness [m]	0.0007
Working pressure [MPa]	Max. 10
Working temperature [℃]	Max. 400, Min. −196
Number of plate	3
Chevron angle [°]	45

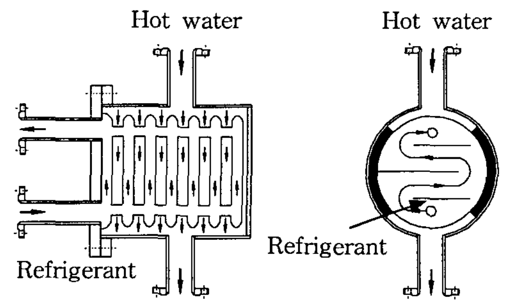

Fig. 3 Details of flow pattern in plate and shell heat exchanger.

2.1.1 Test section

The plate and shell heat exchangers used in this study was formed by three commercialized SUS-304 plates.

The plate surfaces were pressed to become grooved with a corrugated trapezoid shape and 45 deg of chevron angle. The corrugated grooves on the right and left outer plates have an oblique shape but those in the middle plate have a contrary oblique shape on both sides. Due to the contrary oblique shapes between two neighbor plates the flow streams near the two plates cross each other in each channel. This cross flow creates a significantly unsteady and random flow. In fact, the flow is highly turbulent even at low Reynolds number.

2.1.2 Refrigerant loop

The refrigerant loop contains a compressor, a test section (P&SHE), a pre-heater, a strainer, a refrigerant mass flow meter, a dryer&filter, a manual expansion valve, condenser and post-evaporator. The compressor is a 1.72 kW scroll compressor. The refrigerant flow rate can be adjusted by opening the by-pass valve. The refrigerant flow rate was measured by a mass flow meter (Oval, D040S-SS-322) installed between the strainer and receiver with an accuracy of ±0.2%.

The pre-heater is used to evaporate the refrigerant to a specified vapor quality at the test section inlet by transferring heat from R-22 to the electrical heater. The amount of heat transfer from the electrical heater to the refrigerant in the pre-heater is measured from the power meter (YOKOGAWA WT110). The dryer&filter intends to filter the solid particles possibly present in the loop. The pressure of the refrigerant loop can be controlled by varying expansion valve and the temperature of the water loop in the test section and post-evaporator.

2.1.3 Water loop

The water loop in the system designed for circulating hot water through the test section and post-evaporator contain a 100 liter constant temperature water bath with a 5 kW heater and an air cooled refrigerating unit of 3 RT cooling capacity intending to accurately control the water temperature. A 0.37 kW water pump is used to drive the hot water to the test section with specified water flow rate. Another by-pass water valve can also be used to adjust the water flow rate. The accuracy of measuring the water flow rate by the flow meter (Oval, D040S-SS-200) is ±0.2%.

Table 2 Test conditions

Refrigerant mass flux [kg/m^{2}s]	63~120
Heat flux [kW/m^2]	4.0~10.5
System pressure [MPa]	0.6, 0.7

2.1.4 Data acquisition

The data acquisition unit includes a 20 channel NetDAQ 2645A recorder of FLUKE combined with a personal computer. The recorder was used to record the temperature and voltage data. The flow meters, pressure transducers and differential pressure transducer need a power supply as a driver to output and voltage of 0~10 V. The NetDAQ 2645A recorder allows the measured data to transmit to personal computer and then to be analyzed by the computer immediately.

2.2 Experimental procedures

The system pressure is maintained at a specified level by adjusting the water loop temperature and its flow rate. The vapor quality of R-22 at the test section inlet can be kept at the desired value by adjusting the voltage of the pre-heater. The heat transfer rate between the counter flow channels in the test section can be varied by changing the temperature and flow rate in the water loop for the test section. Any change of the system variables will lead to fluctuations in the temperature and pressure of the flow. It takes about 60~120 min to reach statistically steady state at which variations of the time-average inlet and outlet temperatures are less than 0.1℃ and the variations of the pressure and heat flux are within 1% and 5%, respectively. Then the data acquisition unit is initiated to scan all the data channels for 60 times in 5 min.

3. Data reduction

From the definition of the hydraulic diameter, Shah and Wanniarachchi[10] suggested to use two times of the channel spacing as the hydraulic diameter for plate heat exchanger. So we follow this suggestion.

$$D_h \cong 2b \quad \text{for} \quad w \gg b \tag{1}$$

The total heat transfer rate between the counter flows in the test section is calculated from the hot water side

$$Q_{w,h} = m_{w,h} C_{p,w} (T_{w,h,i} - T_{w,h,o}) \tag{2}$$

Then, the refrigerant vapor quality entering the test section is evaluated from the thermodynamic table.

The change in the refrigerant vapor quality in the test section is then deduced from the heat transfer to the refrigerant in the test section,

$$\Delta x = \frac{Q_{w,h}}{m_r \cdot i_{fg}} \tag{3}$$

The average quality in the test section is

$$x_{ave} = x_m = x_i + \frac{\Delta x}{2} \tag{4}$$

To evaluate the friction factor associated with the R-22 evaporation, the frictional pressure drop ΔP_f was calculated by subtracting the pressure losses at the test section inlet and exit manifolds and ports $(\Delta P_f)_{\text{man}}$, the acceleration pressure drop ΔP_a and the elevation pressure drop ΔP_{ele} from the measured total pressure drop ΔP_{exp}.

$$\Delta P_f = \Delta P_{\text{exp}} - (\Delta P)_{\text{man}} - \Delta P_a - \Delta P_{ele} \tag{5}$$

The acceleration and elevation pressure drops were estimated by the homogeneous model for the two phase gas-liquid flow.[11]

$$\Delta P_a = G^2 v_{fg} \Delta x \tag{6}$$

$$\Delta P_{ele} = \frac{gL}{v_m} \tag{7}$$

where v_m is the mean specific volume of the vapor-liquid mixture in the refrigerant channel when they are homogeneously mixed and is given as

$$v_m = [x_m v_g + (1 - x_m) v_f] = (v_f + x_m v_{fg}) \tag{8}$$

The pressure drop in the inlet and outlet manifolds and ports was empirically suggested by Shah and Focke.[8] It is approximately 1.5 times the head due to the flow expansion at the channel inlet

$$(\Delta P)_{\text{man}} \approx 1.5 \left(\frac{u_m^2}{2v_m} \right)_i \tag{9}$$

where u_m is the mean flow velocity. With the homogeneous model the mean velocity is

$$u_m = G v_m \tag{10}$$

Based on the above estimation the acceleration pressure drop, the pressure losses at the test section inlet and exit manifolds and ports, and the elevation pressure drop were found to be rather small. The frictional pressure drop ranges from 93% to 99% of the total pressure drop measured. According to the definition

$$f_{TP} \equiv \frac{\Delta P_f D_h}{2G^2 v_m L} \tag{11}$$

4. Results and discussion

4.1 Single phase pressure drop

Before measuring the R-22 evaporation pressure drop, single phase water to water tests were conducted first. The results from this single phase experiment were illustrated in Fig. 4 and 5 and the measured single phase pressure drop in the plate and shell side can be correlated by the least-square method as

Type A

$$\text{Plate side}: f_l = 1.020\text{Re}^{-0.080} \tag{12}$$

$$\text{Shell side}: f_l = 3.303\text{Re}^{-0.227} \tag{13}$$

Type B

$$\text{Plate side}: f_l = 0.38\text{Re}^{-0.032} \tag{14}$$

$$\text{Shell side}: f_l = 0.92\text{Re}^{-0.167} \tag{15}$$

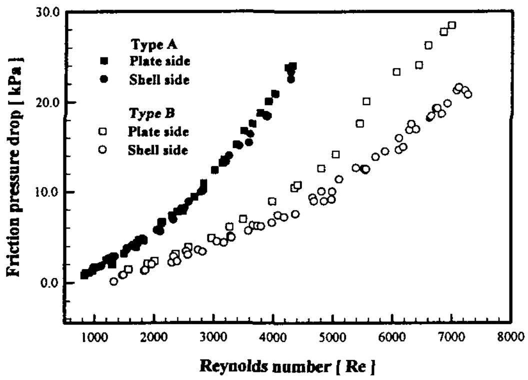

Fig. 4 Experimental results for single-phase flow frictional pressure drop in the plate and shell side.

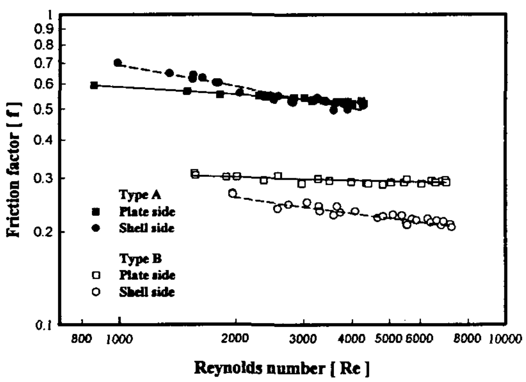

Fig. 5 Experimental results for single-phase flow friction factor in the plate and shell side.

The average deviation is about 3% between the experimental data and the correlation.

4.2 Two phase pressure drop

Effects of the mass flux, heat flux, and system pressure on the evaporation pressure drop of refrigerant R-22 in the two types of the P&SHE were examined in the following.

Measured data are presented in Fig. 6~10 to illustrate the changes of the frictional pressure drop with the vapor quality for various mass fluxes, heat fluxes, and system pressures.

Figure 6 shows the effects of the mass flux on the frictional pressure drop of Type A at an average pressure of 0.7 MPa and an average heat flux of 9.6~10.5 kW/m^2 for the mass flux ranging from 63 to 77 kg/m^{2}s and the mean vapor quality varying from 0.2 to 0.63. The mean vapor quality x_m is the average vapor quality in the P&SHE estimated from x_i and Δx. These data indicate that at a given mass flux the evaporation pressure drop increases with the mean vapor quality of the refrigerant in the P&SHE. Especially, at 77 kg/m^{2}s the evaporation pressure drop at the quality x_m of 0.63 is about 80% larger than that at 0.2. This

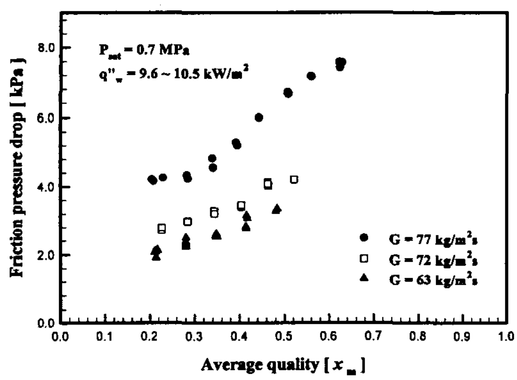

Fig. 6 Frictional pressure drop variation with mean vapor quality for various mass fluxes at P_{sat}=0.7 MPa and q_w''=9.6~10.5 kW/m^2 for Type A.

is attributed to increase in the velocity of vapor at a higher x_m.

The effects of the heat flux on the pressure drop are examined in Fig. 7. Two heat fluxes were tested at a given mass flux of 77 kg/m^{2}s and pressure of 0.7 MPa. Similar to the effect of mass flux, the pressure drop increases with the vapor quality. It is further noted that the higher heat flux results in a higher pressure drop for the entire quality range. Note that the quality-averaged evaporation pressure drops at 9.6~10.5 kW/m^2 are about 25% larger than that at 7.8~8.2 kW/m^2.

Figure 8 presents the data for the evaporation pressure drop at the mass flux 63 kg/m^{2}s and the heat flux 9.6~10.5 kW/m^2 for two system pressures of 0.6 and 0.7 MPa which respectively correspond to the saturated temperatures of 6℃, 11.5℃. In the low-quality regime the pressure effects are small but at the high-quality regime pressure drop is reduced with an increase in the system pressure. It is known that for a higher system pressure, the specific volume of the vapor and the viscosity of the

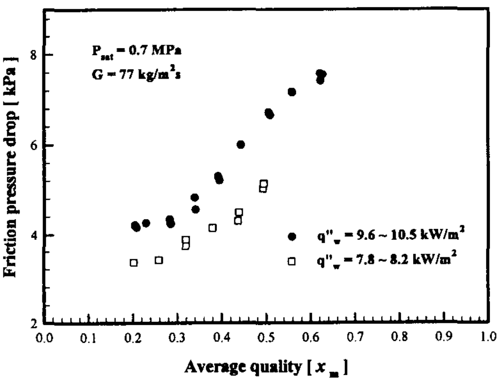

Fig. 7 Frictional pressure drop variation with the mean vapor quality for two different heat fluxes at P_{sat}=0.7 MPa and G=77 kg/m^{2}s for Type A.

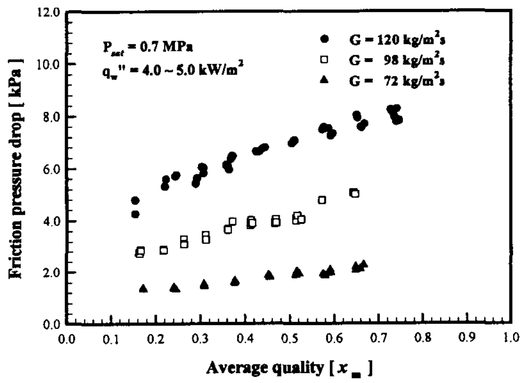

Fig. 9 Frictional pressure drop variation with mean vapor quality for various mass fluxes at q_w'' =4.0~5.0 kW/m^2 and P_{sat} =0.7 MPa for Type B.

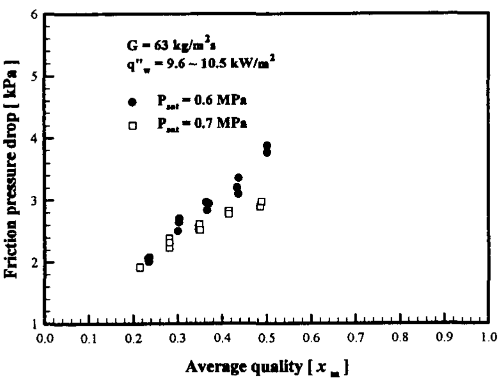

Fig. 8 Frictional pressure drop variation with the mean vapor quality for various system pressures at G=63 kg/m^{2}s and q_w'' =9.6~10.5 kW/m^2 for Type A.

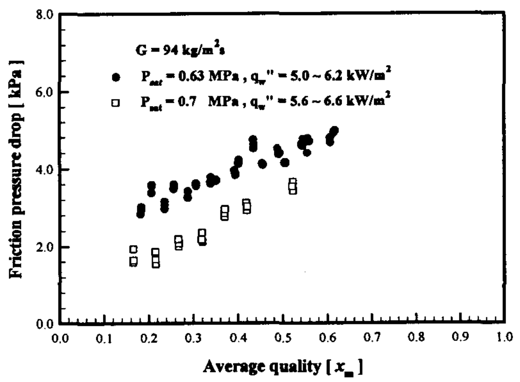

Fig. 10 Frictional pressure drop variation with mean vapor quality for various system pressure at G=94 kg/m^{2}s for Type B.

liquid R-22 are lower.

Figure 9 and 10 present the results of Type B. A similar trend like Fig. 6 is noted in Fig. 9 for the effect of mass flux. At a given mass flux the evaporation pressure drop increases with the mean vapor quality of the refrigerant in the P&SHE.

Figure 10 shows that an increase in the system pressure leads to reduction in the pressure drop.

It is necessary to compare the present data for the friction factor in the P&SHE to those in PHE reported in the literature. Due to the limited availability of the data for PHE with the same ranges of the parameters covered in the present study, the comparison is only possible for a few cases. This is illustrated in Fig. 11, in which our data are compared with correlation of Yan et al.(12)

Though the experimental conditions including mass flow rate, heat flux level, and pressure for these data somewhat different, the comparison clearly shows that the friction factor for P&SHE is about 50% (Type A) and 30% (Type B) in average less than that for the PHE.

This is attributed to flow distribution of port, that is, the flow distribution of port in the P&SHE is better than that of PHE.

To facilitate the use of the plate and shell heat exchangers as an evaporator, correlation equations for the dimensionless two-phase flow friction factor based on the present data are provided. They are

Type A

$$f_{TP} = 7.33\times10^2 \mathrm{Re}_{eq}^{-0.39} \quad 3500 \le \mathrm{Re}_{eq} \le 10000 \tag{16}$$

Type B

$$f_{TP} = 5.58\times10^4 \mathrm{Re}_{eq}^{-0.85} \quad 4500 \le \mathrm{Re}_{eq} \le 11000 \tag{17}$$

where Re_{eq} is defined as

$$\mathrm{Re}_{eq} = \frac{G_{eq} D_h}{\mu_l} \tag{18}$$

in which

$$G_{eq} = G\left[1 - x_m + x_m\left(\frac{\rho_l}{\rho_v}\right)^{0.5}\right] \tag{19}$$

Here G_{eq} was proposed by Akers et al.(13) and is an equivalent mass flux which is a function of the R-22 mass flux, mean vapor quality and densities at the saturated condition. Figure 12 illustrates the comparison of the proposed correlation for the friction factor to the present

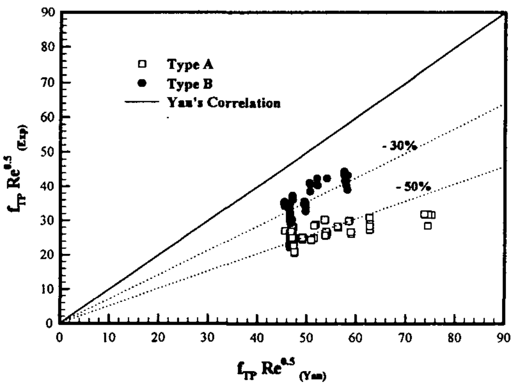

Fig. 11 Comparison of the present friction factor with those for plate heat exchanger from Yan et al.(12)

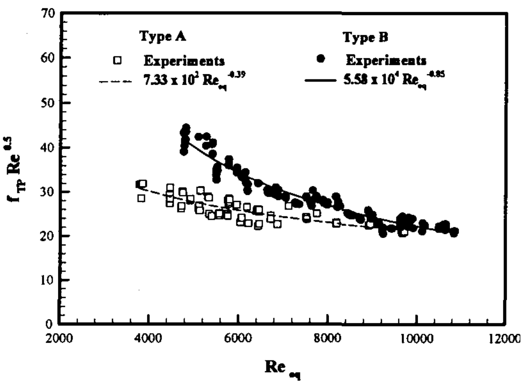

Fig. 12 Comparison of the proposed correlation for the friction factor with the present data.

data. It is found that the average deviation is about 10% (Type A, Type B) between the f_{TP} correlation and the data.

5. Conclusions

An experiment has been carried out in the present study to measure pressure drop for the evaporation of R-22 flowing in the P&SHE. The effects of the mass flux of R-22, average heat flux, system pressure and vapor quality of R-22 on the measured data were experimentally investigated in detail. The results show that the evaporation pressure drop increases with the increment of refrigerant mass flux and heat flux. But a higher system pressure results in a lower pressure drop comparatively. Correlations were also proposed for the measured pressure drops in terms of friction factor.

References

1. Williams, B., 1996, Heat Transfer Savings on a Plate, Heating and Air Conditioning Journal. Apt., pp. 29-31.
2. Kerner, J., Sjogren, S. and Svensson, L., 1987, Where Plate Exchangers Offer Advantages Over Shell-and-Tube, Power, Vol. 131, pp. 53-58.
3. Seo, M. K. and Kim, Y. S., 1999, Experimental Study on Heat Transfer and Pressure Drop Characteristics for Single-Phase Flow in Plate and Shell Heat Exchangers, Korean Journal of Air-Conditioning and Refrigeration Engineering, Vol. 12, No. 4. pp. 422-429.
4. Focke, W. W., Zachariades, J. and Oliver, I., 1985, The Effect of the Corrugation Inclination Angle on the Thermohydraulic Performance of Plate Heat Exchangers, Int. J. Heat Mass Transfer, Vol. 28, No. 8, pp. 1469-1479.
5. Cooper, A. and Usher, J. D., 1983, Heat Exchanger Design Handbook, Chap. 3.7, Hemisphere Publishing, New York.
6. Bounpane, R. A. and Troupe, R. A., 1987, A Study of the Effects of Internal Rib and Channel Geometry in Rectangular Channels, AIChE Journal, Vol. 15, No, 4, pp. 585-596.
7. Bogaert, R. and Bolcs, A., 1995, Global Performance of a Prototype Brazed Plate Heat Exchanger in a Large Reynolds Number Range, Experimental Heat Transfer, Taylor & Francis, No. 8, pp. 293-311.
8. Shah, R. K. and Focke, W. W., 1988, Plate Heat Exchangers and Their Design Theory, in Shah, R. K., Subbarao, E. C., Mashelkar, R. A. (Eds.), Heat Transfer Equipment Design, Hemisphere, Washington, DC, pp. 227-254.
9. Kandlikar, S. G. and Shah, R. K., 1989, Multi pass Plate Heat Exchangers Effectiveness-NTU Results and Guidelines for Selecting Pass Arrangements, ASME J. Heat Transfer, Vol. III, pp. 300-313.
10. Shah, R. K. and Wanniarachchi, A. S., 1992, Plate Heat Exchanger Design Theory in Industry Heat Exchanger, in J. M. Buchlin (Ed.), Lecture Series, No. 1991-04, Von Karman Institute for Fluid Dynamics, Belgium.
11. Collier, J. G., 1982, Convective Boiling and Condensation, 2nd ed., McGraw-Hill.
12. Yi-Yie Yan, Hsiang-Chao Lio and Tsing-Fa Lin, 1999, Evaporation Heat Transfer and Pressure Drop of Refrigerant R-134a in a Plate Heat Exchanger, Transactions of the ASME, J. Heat Transfer, Vol. 121, pp. 118-127.
13. Akers, W. W., Dean, H. A. and Crosser, O., 1958, Condensation Heat Transfer Within Horizontal Tubes, Chem. Eng. Prog. 54, pp. 89-90.
14. Nae Hyun Kim and Jin Pyo Cho, 1999, Experimental Investigation of R-22 Condensation in Tubes with Small Inner Diameter, Journal of Air-Conditioning and Refrigeration, Vol. 7, pp. 45-54.